LAWRENCE
LIVERMORE
NATIONAL
LABORATORY

UCRL-CONF-231778

A brief review of the intensity of lines 3C and 3D in neon-like Fe XVII

Gregory V. Brown

June 14, 2007

20 years of Spectroscopy with the Electron Beam Ion Trap
Berkeley, CA, United States
November 12, 2006 through November 16, 2006

A brief review of the intensity of lines 3C and 3D in neon-like Fe XVII

G. V. Brown

Department of Physics and Advanced Technologies,

High Energy Density Physics and Astrophysics Division,

Lawrence Livermore National Laboratory,

7000 East Avenue, L-260, Livermore, CA 94550, U.S.A.

(Dated: June 13, 2007)

Abstract

X-ray emission from neon-like Fe XVII has been measured with high-resolution spectrometers from laboratory or celestial sources for nearly seven decades. Two of the strongest lines regularly identified in these spectra are the $^1P_1 \rightarrow {}^1S_0$ resonance, and $^3D_1 \rightarrow {}^1S_0$ intercombination line, known as 3C and 3D, respectively. This paper gives a brief overview of measurements of the intensities of the lines 3C and 3D from laboratory and celestial sources, and their comparison to model calculations, with an emphasis on measurements completed using an electron beam ion trap. It includes a discussion of the measured absolute cross sections compared to results from modern atomic theory calculations, as well as the diagnostic utility of the relative intensity, $R = \mathrm{I}_{3C}/\mathrm{I}_{3D}$, as it applies to the interpretation of spectra measured from the Sun and extra-Solar sources.

PACS numbers: 32.30.Rj, 32.30.-r, 32.70.Cs, 52.72.+v, 95.85.Nv, 96.60.P-, 97.10.Ex

The X-ray spectrum from neon-like Fe XVII has one of the most distinct spectral signatures of any ion. It has been observed in laboratory plasmas, the Sun, or in extra-solar sources for nearly 70 years, starting in 1938 with the first identification of Fe XVII X-ray lines in the laboratory [1]. The Fe XVII X-ray spectrum is dominated by eight lines falling in the 13–18 Å wavelength band corresponding to X-rays at ~ 13.9 Å emitted from $3p \rightarrow 2s$ transitions, ~ 15 Å from $3d \rightarrow 2p$ transitions, and ~ 17 Å from $3s \rightarrow 2p$ transitions. The lines are commonly labeled 3A–3H starting at the shorter wavelength [2]. Two of the strongest most distinct lines are the $2p^5 3d_{3/2}\ ^1P_1 \rightarrow 2p^6\ ^1S_0$ resonance line 3C, at 15.01 Å, and the $2p^5 3d_{5/2}\ ^3D_1 \rightarrow 2p^6\ ^1S_0$ intercombination line 3D, at 15.26 Å. These lines are particularly attractive as diagnostics because their wavelength separation is large enough to be resolved by spectrometers with moderate resolving power, and small enough so that errors in spectrometer response are relatively small. In addition, because Fe^{16+} is the dominant Fe ion over a large temperature range, 3C and 3D have been observed in a variety of celestial sources including the Sun, other stellar coronae, elliptical galaxies, and supernova remnants. The diagnostic utility of these lines, however, has been limited by the fact that although many extensive studies have been completed, discrepancies between theoretical calculations and measurements from celestial and laboratory sources persist.

The corona of the Sun is a bright source of Fe XVII X-ray emission. In 1963, using a rocket borne crystal spectrometer, Blake et al. [3] measured the first high-resolution Solar spectrum that included Fe XVII X-ray lines. The spectrometer employed no slits for these measurements, so the spectrum included emission from the entire Solar disk. However, owing to the fact that they were only emitted from well localized active regions, the Fe XVII X-ray lines were relatively well resolved. From these first measurements the relative intensity of the resonance to intercombination line, $R = I_{3C}/I_{3D}$, was measured to be 1.60 ± 0.32. Later rocket borne experiments included a collimated Bragg crystal spectrometer that produced some of the highest resolution Fe XVII X-ray spectra ever recorded [2, 4]. The ratio R for these rocket flights ranged from 2.1 to 2.6. The measured ratios were compared to several theoretical calculations, and moderate agreement was found. For example, using calculations based on the Coulomb-Born approximation, Loulergue & Nussbaumer [5] found a ratio R of 2.7, just above many of the observed ratios.

The first satellite borne X-ray spectrometers to measure and resolve the strong Fe XVII X-ray lines were also flown in the 1960s. These were NASA's Orbiting Solar Observatories,

OSO-III, V, and VI [6, 7], and also the United States Air Force's OV1-10 and OV1-17 [8, 9][81]. These satellites all carried slit-less crystal spectrometers that, like early rocket experiments, integrated over the entire Solar disk. These flights were very successful and yielded many high-resolution spectra of Fe XVII [6–10]. From these observation, R was found to lie between 1.8 and 3.2, with larger values generally found in the spectra measured during flares.

In the late 1970s, the P78-1 satellite was launched by the USAF. It carried a Bragg crystal spectrometer with a 20 arcsecond collimation and an RAP crystal for diffraction of X-rays [82]. Rugge et al. [11] compare values of R from 53 observation of the Sun measured by P78-1 between 1978 and 1979, and covering a wide range of Solar activity. These observations included regions with temperatures between 2.5×10^6 and 5×10^6 K. Except for a few outliers, all the values of R from these observations were between 2 and 2.5.

In 1980, the Solar Maximum Mission (*SMM*) was launched. It provided high-resolution spectra of the Sun from 1980 until 1989, a time that covered a peak in Solar Activity [83]. *SMM*'s flat crystal spectrometer had a 14 arcminute collimation and used a KAP crystal to disperse X-rays. Many high resolution spectra were measured using *SMM*; some can be found in Phillips et al 1982 [12], 1997 [13], and 1999 [14], and also Schmelz et al. 1996 [15]. Similar to the P78-1 observations, compilations of several of the values R have been reported [16–19] and R was found in the range from values just below 2 to ~ 2.7.

In 1985, Smith et al. [20] published the results of a more complete calculation of the Fe XVII X-ray emission that, unlike Loulergue & Nussbaumer [5], included configuration mixing in its treatment of the wavefunctions, and also indirect population processes such as dielectronic recombination and resonance excitation. Their results predict R to vary from 3.0 at $2 \times 10^6 K$ to 3.4 at $5 \times 10^7 K$. Comparing these calculations to the results from P78-1, Rugge et al. [11] found that, not only were most of the observed ratios R below theory, but also that other ratios involving line 3C also did not agree with theory. Based on these comparisons, Rugge et al. suggested that, because of its relatively large oscillator strength, the flux of the line 3C was being absorbed then re-radiated out of the line of sight of the detector; a process known as resonant scattering. Several authors took advantage of this effect. For example, Schmelz et al. [16, 21], Saba et al. [17], and Waljeski et al. [22], used resonance scattering of 3C to determine the column density, and electron density of the source, as well as the optical depth of the line 3C. Schmelz et al. [16] also determined that

the opacity of line 3C increased as the distance from the center of the Solar disk to the limb. Phillips et al [19] analyzed the same data set and found the opposite trend in opacity, i.e, the opacity of 3C decreased from center to limb. Saba et al. [17] and Bhatia & Saba [18], revisited the *SMM* data and their analyses agreed with the findings of Schmelz.

Although the original suggestion of resonant scattering by Rugge et al. [11] was based on comparison with the theory of Smith et al [20], Schmelz et al., Saba et al., and Waljeski et al. based their diagnostics on more recent calculations by Bhatia & Doschek [23], and also from Cornille et al. [24]. Bhatia & Doschek and Cornille et al. calculated $R > 4$ for coronal temperatures, larger than the results of Smith et al. [20]. However, many other calculations of the Fe XVII X-ray line intensities had also been completed throughout the 1980s and 1990s [18, 25–28], and values ranging from ~ 3 to nearly 5 were reported. The large variation in the calculations precluded the use of either the intensity ratio, R, or the intensity of line 3C as a dignostic. This variation demonstrated the need for an accurate laboratory value that could be used to benchmark theory and provide a reliable optically thin value for R, which in turn could then be used as a reference for diagnosing celestial sources.

Many laboratory measurements of the Fe XVII X-ray spectrum had been completed up to the 1990s, beginning with the vacuum spark measurements by Tyrén 1938 [1], mentioned earlier. Vacuum spark measurements were also carried out throughout the 1960s and 1970s [29–31] and R was measured to be between 1.1 and 1.6. However, because of the relatively high densities ($n_e \sim 10^{19} cm^{-3}$), and the fact that several charge states are present simultaneously, the low ratios might result from opacity effects and possibly line blending with X-ray emission from other charge states. Fe XVII has also been observed in laser produced plasmas [32–35]; however, those suffer the same problems of high density and presence of many ions as found in vacuum spark plasmas. For example, figure 1 shows 3 different spectra measured from laser produced plasmas at Tor Vergata University [35], where lower charge states are present and opacity effects play a role .

Unlike laser produced and vacuum spark plasmas, plasmas created in tokamaks have densities and temperatures similar to those found in the Solar corona, and, therefore, provide a better means for understanding the atomic processes that produce Fe XVII in the corona. Several measurements that include Fe XVII have been completed using the Princeton Large Torus (PLT) [36, 37], the Divertor and Injection Tokamak Experiment (DITE), and the Joint

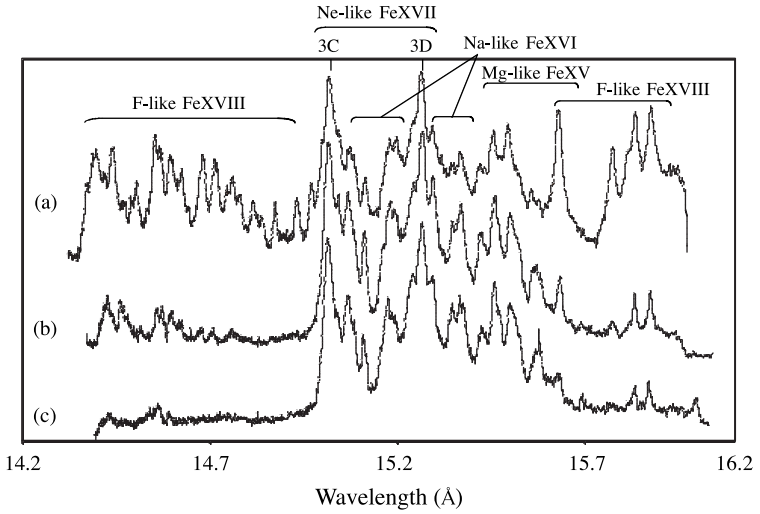

FIG. 1: X-ray spectra of Fe spanning the range between 14 and 16.8 Å. These spectra were obtained from plasmas produced using the 15 ns Nd:glass laser located at Tor Vergata University. Spectra a, b, and c were measured from plasmas produced using different laser energies and spot sizes. (a) laser pulse energy 6 J, laser spot 200 μm; (b) laser energy 4 J, laser spot 500 μm; (c) laser energy 2 J, laser spot 500 μm. The resolving power of the spectrometer used to measure this spectrum was $\lambda/\Delta\lambda \approx 4000$. This figure is adopted from May et al 2005 [35].

European Torus (JET) [13]. R values ranging from 2.05 to 3.33 have been reported [36], similar to values reported from the Sun. Although these ratios are from spectra measured from a multi-temperature plasma, making it challenging to isolate specific atomic processes, and the measured spectra include emission from multiple charge states and ion species, they provide a platform where opacity does not affect the line 3C. For example, from the tokamak results, serious doubt was cast on the presence of resonant scattering in the Solar corona. Figure 2 shows a spectrum of the Fe XVII X-ray lines measured from PLT [36].

In pursuit of understanding the processes responsible for its line intensities, Fe XVII has been investigated using electron beam ion traps (EBITs). Studies using EBITs have several advantages over laser produced plasmas, vacuum sparks, and tokamaks. An EBIT uses a mono-energetic electron beam, making it possible to isolate a single Fe ion species for study, and to probe specific population processes. EBITs operate at densities of $2 \times 10^{10} - 5 \times 10^{12} cm^{-3}$, similar to many celestial sources. Also, no opacity effects are present in EBIT measurements that may affect the line intensities of Fe XVII 3C or 3D. In all, EBITs provide a stable, low-background source of X-ray emission making it possible to measure

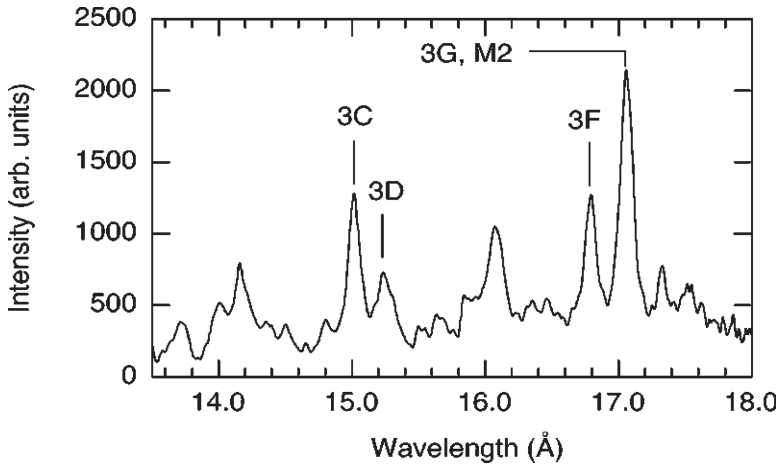

FIG. 2: Spectrum measured at the Princeton Large Torus (PLT) tokamak. This is the sum of several different tokamak runs, and was measured using a rotating flat-crystal spectrometer with a microchannel-plate readout [36].

high resolution, high signal-to-noise spectra under well controlled conditions.

In 1993, in anticipation of the launch of the *Chandra* and *XMM-Newton* X-ray observatories, the laboratory astrophysics program centered around Lawrence Livermore National Laboratory's electron beam ion traps began. The goal of this program was to provide accurate, complete sets of atomic data including wavelengths, line identifications, and excitation cross sections and rate coefficients for astrophysically relevant ions, with a strong emphasis on the Fe L shell ions. As part of these studies, many novel methods of operating the LLNL EBIT were invented and refined in order to help with the interpretation of high resolution X-ray spectra from celestial sources. To name a few, these include the ability to produce a quasi-Maxwellian distribution of electron energies [38, 39], and the ability to study spectra produced by charge exchange recombination using the magnetic trapping mode [40, 41]. The LLNL EBIT facility enjoys a suite of spectrometers for measuring photon emission, including crystal spectrometers [42–44], grating spectrometers [45], solid state detectors, and the NASA/GSFC microcalorimeter array [46–48]. The flexibility and wide range of parameter space available to the EBITs make them perfectly suited for benchmarking atomic theory and for providing accurate, complete sets of atomic data for interpreting astrophysical spectra. A detailed description of the LLNL EBIT facility, including its utility as a tool for laboratory astrophysics, can be found elsewhere [49–51].

To provide the basis for understanding the atomic processes governing the Fe L-shell

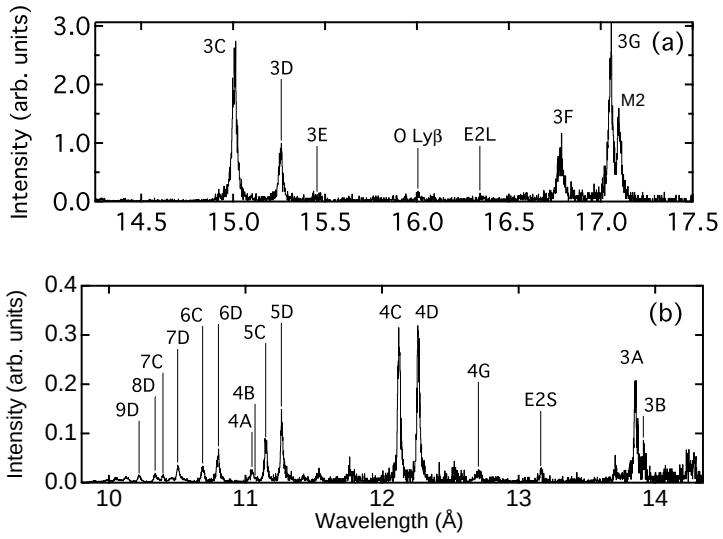

FIG. 3: Fe XVII first-order spectra measured using the LLNL EBIT-II and a flat crystal vacuum spectrometer [52]. Lines 3C and 3D are easily resolved.

.

transitions and to maximize their diagnostic potential, the laboratory astrophysics program at the LLNL EBIT facility began with studies of Fe L-shell X-ray emission, with Fe XVII being the first [52]. The Fe XVII L-shell studies were largely completed using flat crystal Bragg spectrometers [42, 43]. These spectrometers employed TLAP, KAP, or RAP crystals and gas-filled position sensitive proportional counters for the detection of photons and had a resolving power of $\lambda/\Delta\lambda \approx 500$ at 15 Å. The Fe XVII studies produced accurate wavelengths for 29 Fe XVII lines and included the identification of weak, high-n to $n = 2$ transitions up to $n = 14$. Figure 3 shows the first-order spectrum measured at EBIT spanning the 10–17.5 Å band, and Figure 4 gives the second order spectrum showing the high-n transitions. In addition to the wavelengths and line identifications, this work demonstrated that the flux contribution from high-n transitions accounts for a significant amount of the total flux emitted from Fe XVII. This flux had been missing from the spectral modeling packages and its inclusion accounted for the "missing flux" problem found in the analysis of some *ASCA* data. Wavelengths from this study have been implemented in standard spectral modeling packages, such as APEC [53], employed by the high-energy astrophysics community for analyzing X-ray spectra.

Several independent measurements of R using different crystals and several different

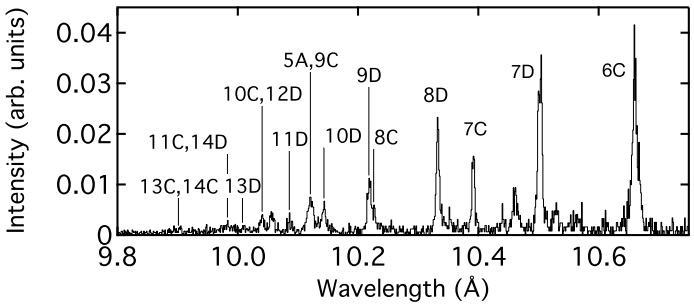

FIG. 4: Second-order spectrum of Fe XVII X-ray line emission used to determine flux of high-n Fe XVII transitions [52].

.

mono-energetic electron beam energies were completed as part of the LLNL EBIT Fe XVII study. For these measurements, the only population processes available were direct excitation from the ground state, resonance excitation, and population by radiative cascades from higher lying levels. For impact energies between 850 eV and 1300 eV, the average value of R was measured to be 3.04 $\pm$ 0.12 [52]. As a check on this result, R was measured along the neon-like isoelectronic sequence for elements with Z between 24 and 36 [54](see figure 5 and also Beiersdorfer et al. [36]). The Fe result agrees with the observed dependence of R on atomic number, validating the Fe XVII measurement and also demonstrating that the overestimation by theory is consistent along the entire neon-like isoelectronic sequence for mid-Z ions. The LLNL EBIT value of R is well below the calculated value adopted by the Solar physics community when assessing the influence of resonance scattering. However, it is in agreement with many, but not all, of the values measured from the Sun, indicating that in some cases no scattering occurred and in others its effect had been overestimated.

In pursuit of the cause of the ratios observed in Solar corona that were lower than the LLNL laboratory measurements, the laboratory study was expanded to include measurements of R in the presence of large abundances of Na-like Fe XVI to measure the influence of Na-like Fe XVI innershell satellite lines that fall near the line 3C and 3D [56]. Because the energies required to excite the innershell satellites are much greater than the 489 eV ionization potential of Fe XVI, and at these higher energies the charge balance in the LLNL EBIT is nearly 100% Fe XVII when using the MeVVA for injection, a different injection method was used. Specifically, neutral Fe was injected as gaseous iron pentacarbonyl, $Fe(CO)_5$.

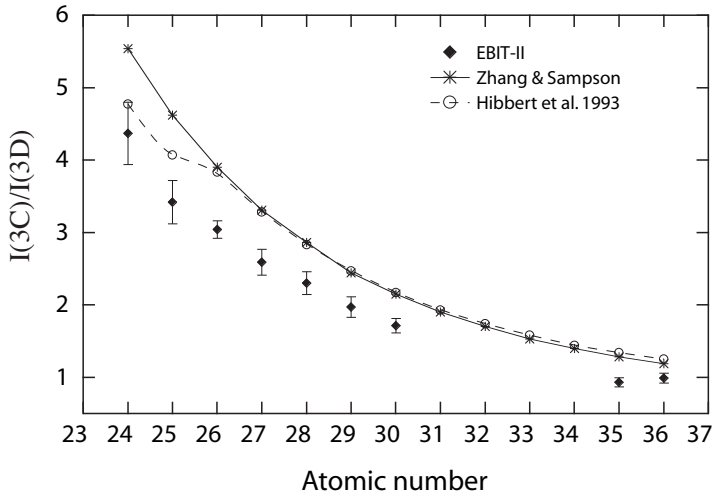

FIG. 5: Comparison of measured and calculated relative intensity, R, as a function of Z along the neon-like isoelectronic sequence. Measured values, labeled EBIT-II, are compared to calculations of Hibbert et al. [28] and Zhang & Sampson [55] . This figure is adopted from from [54].

.

By injecting iron in gaseous form, the average charge in the trap was reduced and a large fraction of Fe XVI was present in the trap in addition to Fe XVII, and at energies above the threshold for exciting Fe XVI innershell satellites. These measurements unveiled the fact that an Fe XVI innershell satellite line is coincident with the Fe XVII intercombination line 3D, causing lower values of R when large amounts of Fe XVI are present (see figure 6). It followed that in other sources, where significant amounts of Fe XVI and XVII coexist, the ratio R is reduced by the enhancement of line 3D by the coincident line "C" from Na-like Fe XVI. This line coincidence explained the low ratios measured in tokamaks [36]. In addition, by coupling the relative abundance of Fe XVI to Fe XVII to its temperature dependence and then the strength of line C to the Fe XVI abundance, Brown et al. [56] showed that R can be used as a temperature diagnostic. Figure 7 graphs the electron temperature versus apparent ratio R.

Measurements of Fe XVII X-ray emission have also been completed using the electron beam ion trap located at the National Institute of Standards (NIST) using a single pixel microcalorimeter provided by the Harvard-Smithsonian Center for Astrophysics. In those

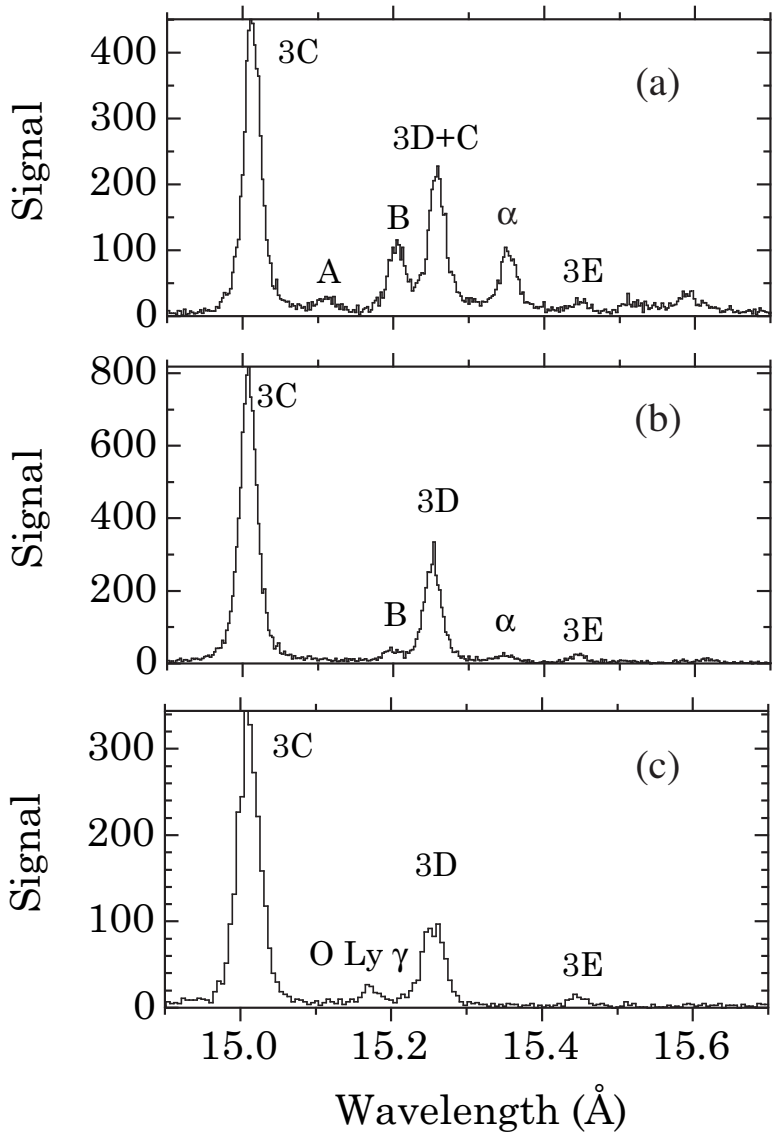

FIG. 6: Fe L-shell spectra measured for different relative abundances of FeXVI relative to Fe XVII. (a) relative abundance of ≈ 1 (b)relative abundance of ≈ 0.15; (c)only Fe XVII. Figure (c) shows the standard (equilibrium) ionization balance obtained by iron injected with the MeVVA. This figure is from Brown et al. [56].

experiments, the ratio was measured at two different electron beam energies. The ratios measured were 2.94 ± 0.18 for a beam energy of 900 eV and 2.50 ± 0.13 for a beam energy of 1250 eV [57]. Because of the relatively low resolving power of the SAO instrument ($E/\Delta E \sim 90$ in the 700–900 eV band), the fact that no attempt was made to "gate out" the transient phase of the NIST EBIT cycle time, and that no simultaneous high resolution spectrum was measured, the amount of contamination from Na-like Fe XVI in the SAO

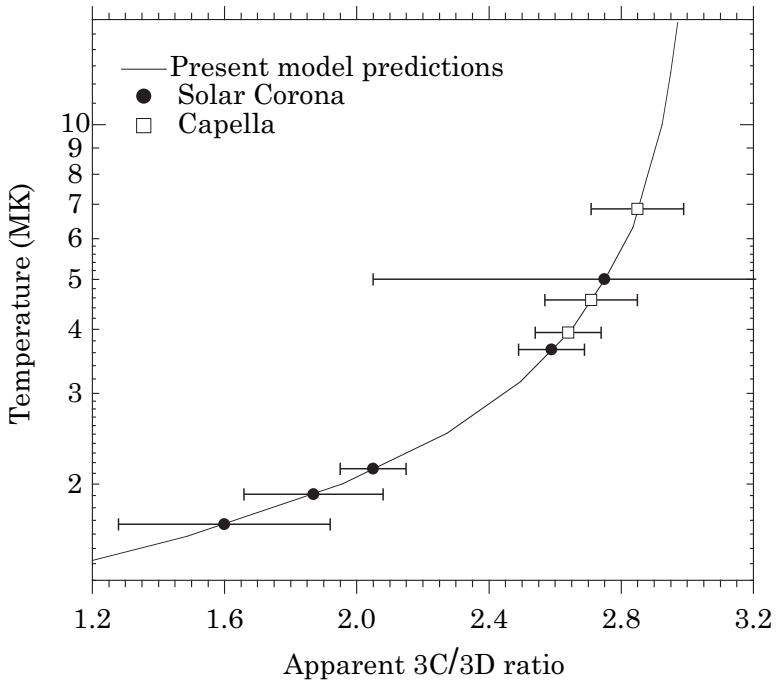

FIG. 7: Correlation of the apparent 3C to 3D ratio with the electron temperature. This curve is based on the ion balance calculations of [58]. Also shown is the predicted temperatures based on the measured ratios R for Capella and for regions of different activity in the Sun. This figure is from Brown et al. [56].

calorimeter spectrum is unknown.

Motivated by the laboratory astrophysics work, Brickhouse & Schmelz [59] revisited the values of R measured by *SMM* to determine the effect of the Fe XVI innershell satellite line coincident with 3D. They found that R does increase as a function of electron temperature, that the low ratios are explained by the presence of Fe XVI line coincidence, and that, unlike in previous analyses, invoking resonant scattering was not necessary. Figure 8 compares the spectrum measured at the LLNL EBIT in the presence of a large amount of Na-like Fe XVI to one of the spectra measured using SMM. The Fe XVI innershell satellites are clearly seen in both spectra.

Using the reflection grating spectrometer (RGS) on *XMM-Newton* and the transmission grating spectrometers (HETG and LETG) on *Chandra*, high resolution spectra of Fe XVII have been measured from a variety of extra-Solar sources, particularly stellar coronae, and lines 3C and 3D have been measured and resolved, in most cases for the first time [60–64]. One of the standard sources observed by both *Chandra* and *XMM-Newton* is the binary

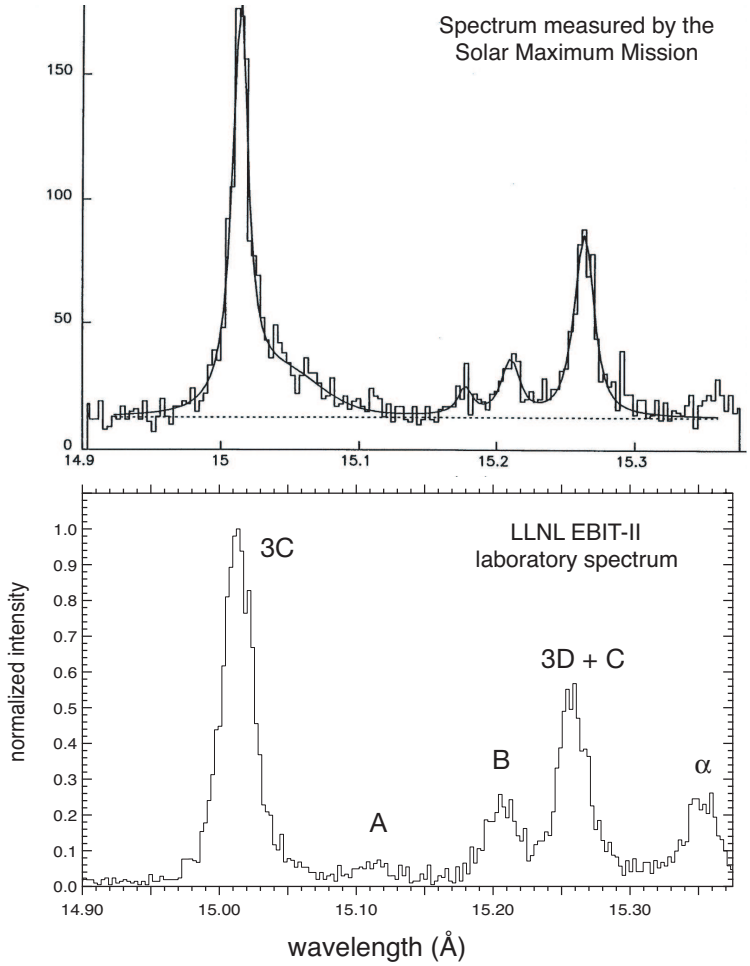

FIG. 8: Comparison of Solar spectrum and spectrum measured at LLNL EBIT. The low ratios measured at LLNL in the presence of relatively large amounts of Fe XVI indicated that the Fe XVI innershell satellite line "C" is coincident wit the Fe XVII intercombination line 3D, and was responsible for the low ratios found in the Sun. The lines labeled "A" and "B" are also Fe XVI innershell satellites, and line "α" is an Fe XVI innershell satellite. The top figure is adopted from Brickhouse & Schmelz [59] and the bottom is adopted from Brown et al. [56].

star Capella (see figure 9). For Capella, the HETG measured a value of 2.72 ± 0.06 [61], and the LETG measured a value of 2.64 ± 0.10 [62]. In the analysis of Capella data, the presence of the line coincidence of the Na-like line "C" and the Fe XVII line 3D was pointed out by Behar et al. [65] independently of the measurements by Brown et al. [56]. Ness et al [60] did an extensive study of the ratio measured from 24 different stellar coronae using measurements from both the RGS and HETG, and found R to be in the same range as measured in the corona of the Sun. Although many sources have ratios that are comparable

to those measured at the LLNL EBIT and thus no significant resonance scattering is taking place, resonant scattering of line 3C has been observed (see for example [63]). Hence, when diagnosing a plasma using R the influence of Ne-like Fe XVI must be accounted for before a determination of the amount of scattering can be made, and before using R as a temperature diagnostic, the possibility of resonant scattering must be assessed.

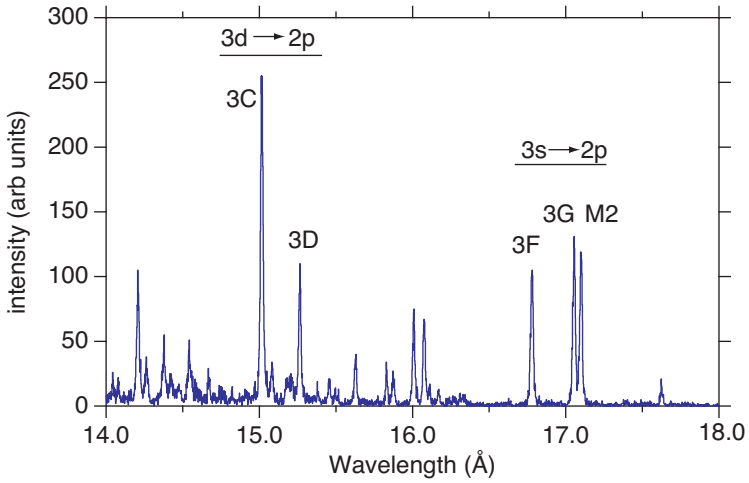

FIG. 9: *Chandra* spectrum of Capella taken with the High Energy Transmission Grating (HETG). The five strong neon-like $3 \rightarrow 2$ transitions are labeled 3C, 3D, 3F, 3G, and M2. The lines are grouped by transition type. 3C and 3D are produced by $3d \rightarrow 2p$ transitions, and the 3F, 3G, and M2 are produced by $3s \rightarrow 2p$ transitions.

The studies of Fe XVII at LLNL also include the intensity of the $3s \rightarrow 2p$ lines relative to 3C [37, 66]. These measurements were conducted using three different instruments: a crystal spectrometer, a grating spectrometer, and a microcalorimeter spectrometer array built by the NASA/Goddard Space Flight Center, and were conducted at 13 different electron impact energies. Similar to the results for R, the $I_{\Sigma(3s\rightarrow 2p)}/I_{3C}$ line ratios agree with observations from celestial sources and tokamaks, but are much larger than theoretical calculations. Figure 10 shows the results of these measurements compared to ratios observed in celestial sources and also compared to calculations [66]. The discrepancies found between theory and measurements for these ratios, along with the discrepancies found between theory and measurement for R, lead Beiersdorfer [37] to suggest that, since resonant scattering has been eliminated as the source for the disagreements with ratios involving line 3C, the problem must lie in the underlying atomic physics used in the calculations of the 3C line strength.

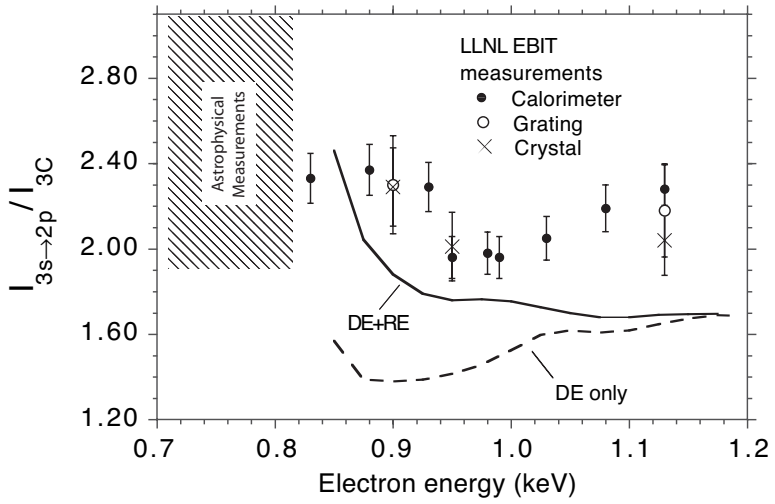

FIG. 10: Relative intensity given by $\Sigma(3s \rightarrow 2p)/3\mathrm{C}$ vs electron energy compared to model calculations using the Flexible Atomic Code (FAC) code [67] with and without resonant excitation, shown as solid and dashed lines, respectively. Both are convolved with a 30 eV spread in the electron beam energy. The hatched region on the left represents the range of values measured from astrophysical sources, and in these cases, the lines may be emitted over a range of temperatures, so that the location in electron energy is not especially clear. The energy scale on the x-axis should, therefore, be disregarded for these. This figure is adopted from [66].

The agreement found between laboratory measurements and the high-quality observational results provided a strong impetus for another generation of more advanced calculations of the Fe XVII X-ray lines, and many have been completed [67–72]. In some of these cases, marginal to good agreement with the experimental ratio R was found, although different methods of calculation were used and the reasons for why now better agreement was found differed between the different calculations. For example, Chen & Pradhan [69] and Loch et al. [72] used a closed-coupling, R-matrix calculation, including an extensive set of resonance excitation channels, to find agreement at energies where resonances are known to exist, while Fournier & Hansen [71] used a distorted wave approach with improved configuration-interaction coefficients based on laboratory values of the level energies. Chen & Pradhan [69] argued that resonance excitation plays a strong role in the total cross section and discrepancies between theory and measurements are a result of the fact that many

calculations do not include resonance excitation or underestimate its contribution. Indeed, their ratio agreed with the laboratory results at some energies where resonances play a role. However, strong contributions from resonance excitation were not borne out by other calculations and the ratios predicted by [69] do not agree with measurements at higher energies where resonance do not play a role (see figure 11). Because ratios from celestial sources are emitted from plasmas containing a distribution of Fe ions, multi-ion models have also been employed in an attempt to reproduce the observed ratios [67, 68]. While these models did find that population processes involving other ions bring the ratio involving the $3s$ lines into better but not complete agreement, in the case of the the ratio R, essentially no effect was seen (excluding the influence of the coincident innershell Fe XVI line mentioned above).

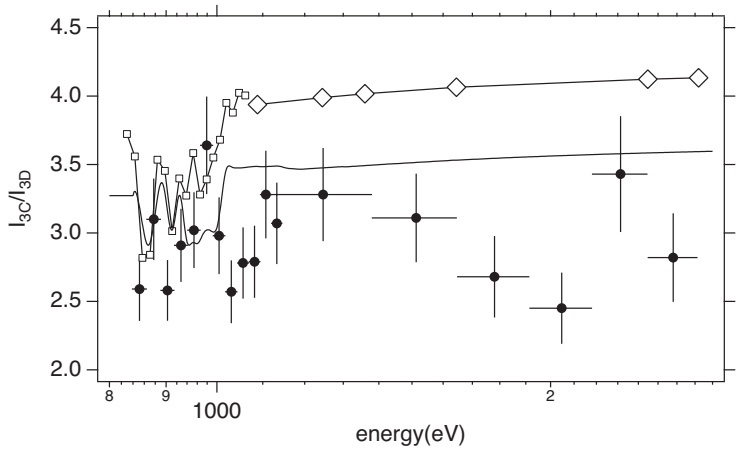

FIG. 11: Measured relative intensity $R = \mathrm{I}_{3C}/\mathrm{I}_{3D}$ versus electron impact energy compared to the theory of of [27] (solid line with open diamonds), [69] (solid line with open squares), and the FAC calculations with resonance excitation (solid line). Although some calculations agree in the region where resonance excitation is present, the results are significantly larger than measured at higher energies.

The challenge of unraveling the mystery of the relative line intensities of the neon-like Fe XVII lines requires a set of measurements that goes beyond relative intensities, i.e., it requires a measurement of the absolute cross sections. Complete sets of absolute excitation cross sections provide the most stringent test of theoretical calculations and also can provide the basis for accurate excitation rate coefficients necessary to model X-ray emission from a variety of plasmas. Essentially, the LLNL EBIT was built specifically to measure absolute cross sections; however, the low resolution of solid state detectors and the prohibitively low

effective collecting area of crystal spectrometers have limited these measurements of L-shell transitions of high Z ions or K-shell transitions in low to mid Z ions [73, 74]. In these cases, the uncertainty in the unknown overlap between the source ions and the electron beam can be avoided by simultaneously measuring the photon emission from radiative recombination (RR) of beam electrons with source ions.

The implementation of NASA/Goddard Space Flight Center's X-ray microcalorimeter, the EBIT/XRS [46–48], at the LLNL EBIT facility in 2000 provided the resolution and collecting area necessary to measure the absolute excitation cross sections of Fe L-shell X-ray line emission. Because of its large bandwidth and energy resolution of $\leq$ 10 eV, this instrument is able to resolve and detect photons from both direct excitation and radiative recombination simultaneously, eliminating cross calibration errors. Since 2000, the absolute cross sections of the X-ray lines from all the Fe L-shell ions, Fe XVII–Fe XXIV have been measured [75–77]. These measurements were done as a function of electron impact energy and in many cases go from energies below excitation threshold where dielectronic resonances contribute, to above threshold where direct excitation from the ground state, resonance excitation, and cascade contributions can contribute to the line strength. Figure 12 shows the measured spectra used to determine the absolute cross sections of line 3C and 3D, including a high resolution crystal spectrum of the direct excitation line emission used to check for line blending. The high resolution of the XRS/EBIT made it possible to measure level specific RR into the 3s, 3d, and 3p levels and the excitation cross sections, σ_{3C} and σ_{3D}, are determined from normalizing to each RR peak independently. The agreement found between the cross sections derived from each peak [77] shows that no influence from background ions or high-lying DR channels influenced this result.

Figure 13 shows the results of the cross section measurements for lines 3C and 3D compared to the R-matrix calculations of [78] and [27], and the distorted wave calculations using the FAC. Oddly, the R-matrix calculations of [69], which are believed to be more complete and accurate because they include resonances in an *a priori* fashion (and which gave good agreement with the measured R ratio at a few electron impact energies), gives discrepant results for the cross sections of both 3C and 3D. The LLNL measurements show that the cross section for line 3C, the resonance line, is significantly smaller than predicted, while better agreement is found for the intercombination line, 3D. In fact, excellent agreement is found between the EBIT measurements and calculations of the 3D cross sections when

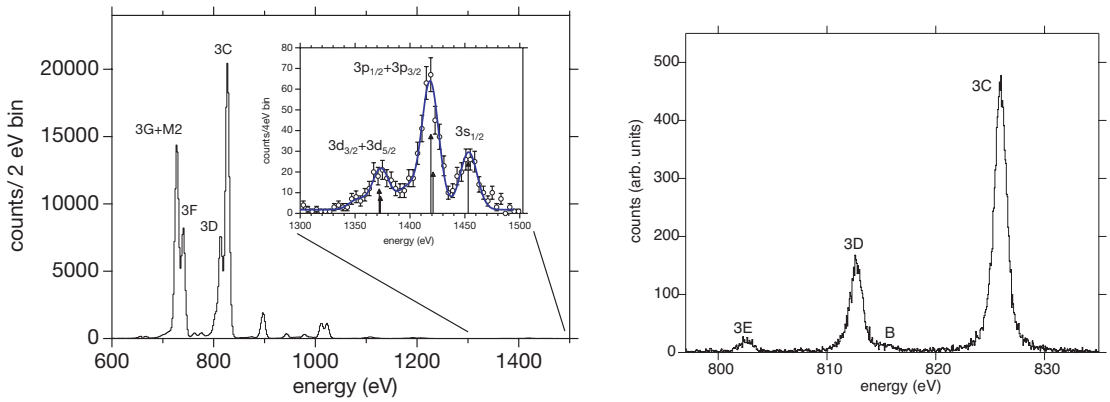

(A) **(B)**

FIG. 12: (A) Spectrum of Fe XVII measured by the XRS/EBIT. The insert shows a close up view of the energy range containing the photons from M-shell radiative recombination. The width of the RR peaks is 20 eV FWHM, and is determined by the width of the electron beam energy. The peaks are labeled with their different fine structure levels. (B) Crystal spectrum measured simultaneously to insure no line blending influences the cross sections for the DE lines measured with the microcalorimeter. Line B is the strongest innershell satellite line from Na-like Fe XVI.

no resonances or cascades are included in the model. Not surprising, is that EBIT measurements show resonances contribute little to the total cross section of either 3C or 3D, in agreement with most theories. This result illustrates the importance of absolute cross section measurements; measurements involving only ratios are clearly not stringent enough to constrain theory, and also demonstrates that the discrepancies found between theory and experiment in the of line 3C, are rooted in the calculation of the direct excitation cross section.

The fact that the cross section measurements agreed well with the values assumed by astrophysical spectral modeling codes for 3D explains the fact that when modeling spectra from the stellar corona of Capella [65], better agreement was found when normalizing to the line strength of the intercombination line 3D. Normalizing to 3C gave poor spectral modeling results, which is expected from the finding that atomic theory does not accurately predict the excitation cross section needed for predicting the intensity of this line.

The large discrepancy between theory and measurement in the case of σ_{3C} and σ_{3D}, as

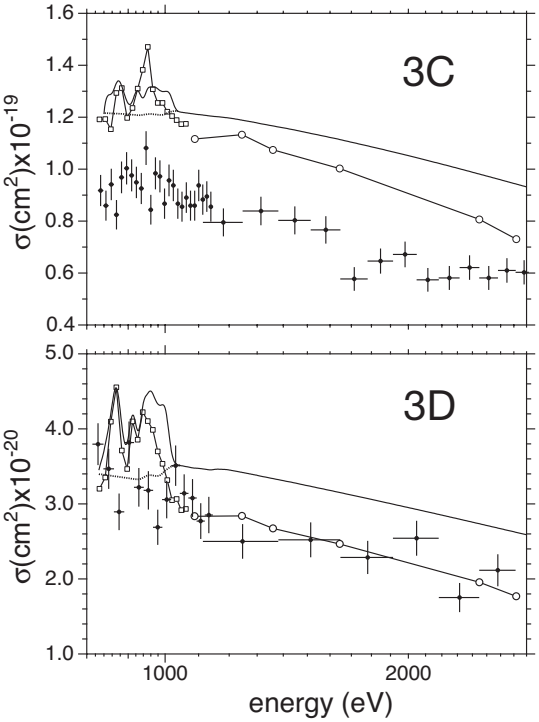

FIG. 13: Cross sections for the resonance line 3C (top) and intercombination line 3D (bottom) as a function of electron-impact energy given by closed circles. The error bars in the y direction are statistical and the error bars in the x direction denote the bin size. These curves are normalized to the single-energy measurement at E_{e-}= 964 eV. Each cross section is compared to the theories of [27] (solid line with open circles), [69] (solid line with open squares), and the FAC calculations with (solid line) and without (dotted line) resonance excitation.

well as the discrepancies found in the various relative line intensities, has sparked interest in the X-ray emission from other neon-like ions, namely neon-like Ni XIX. The study of Ni XIX, although not as mature, has followed a similar path as Fe XVII. The measured ratio R for Ni XIX has been found to be significantly lower than calculated [54]. A more complete follow-up study [79] of all of the strong Ni XIX X-ray line emission, including extensive modeling and measurements, support the discrepancies found by [54], and also found the measured relative intensities of the $3s \rightarrow 2p$ lines relative to 3C, as in the Fe XVII case, to be larger than predicted (see figure 14). Again, similarly to the case of neon-like Fe XVII spectrum, an extensive set of R-Matrix calculations of the relative cross sections of the resonance to intercombination lines 3C and 3D have been completed [80], and some agreement was found with EBIT experiments (see figure 15). Because no experimental values for the absolute

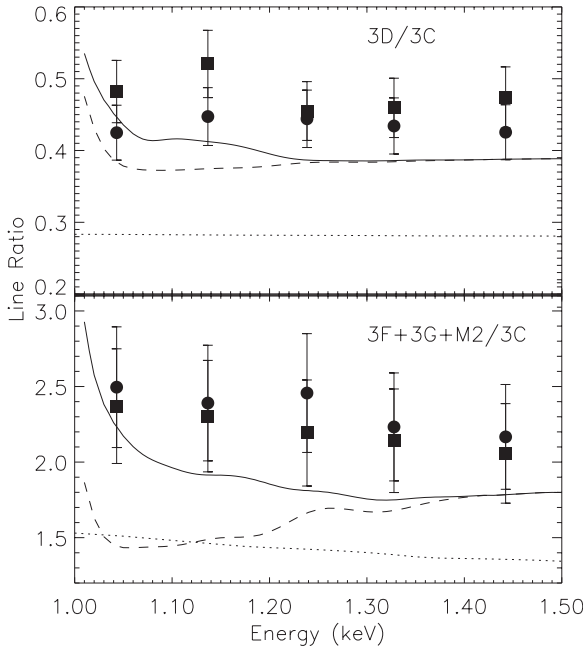

FIG. 14: Comparison of the experimental and theoretical Ni XIX line ratios. The filled circles are measurements from the grating spectrometer, and the filled squares are those from the NASA/GSFC XRS/EBIT microcalorimeter. All the experimental data were measured at the LLNL EBIT facility. The solid lines are the theoretical calculations using the Flexible Atomic Code (FAC) which includes resonance excitation. The dashed lines are from FAC without resonance excitation. The dotted lines are ratios from APEC for Maxwellian plasmas with temperatures in the 500–1000 eV range, i.e., for APEC, an energy of 1 keV in the figure corresponds to a temperature of 500 eV. These plots are from Gu et al 2004 [79].

cross sections of the Ni XIX lines exist, there is no way to know if the calculations of [80] are as good as implied by the comparison with the R ratio, or if the agreement found with the relative intensities is fortuitous, as it was in the Fe XVII case. To check the cross sections of the Ni XIX lines 3C and 3D, measurements of the absolute excitation cross sections have been planned. These measurements would not only test the validity of the agreement between theory and experiment in the case of the intensity ratios, but would also provide a consistency check on the measured absolute excitation cross sections, σ_{3C} and σ_{3D} of Fe XVII. This check would provide more evidence of the finding that, in the case of line 3C, the discrepancies between theory and experiment lie in the calculation of the direct excitation cross section.

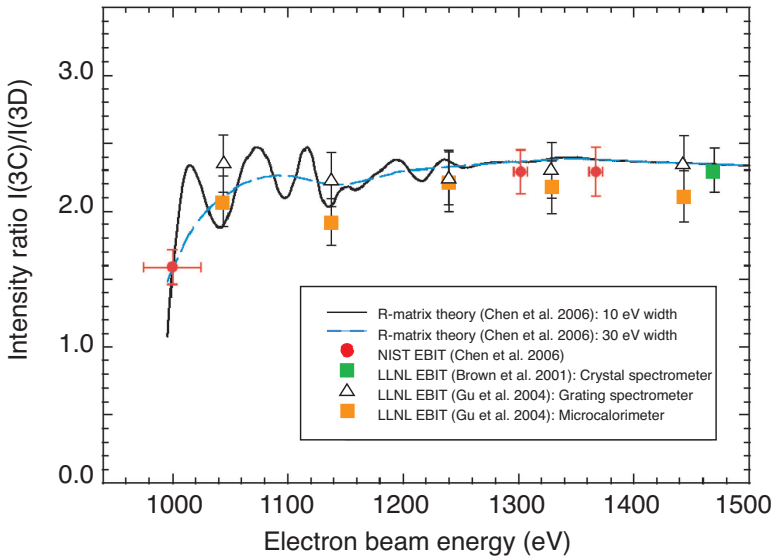

FIG. 15: Measured ratios of the relative intensities of the lines 3C to 3D in Ni XIX compared to the calculations of Chen et al. [80]. The detailed R-matrix calculations of Chen et al., which include an extensive set of resonances, are averaged over two different gaussian beam widths (FWHM), 10 eV and 30 eV. The oscillatory behavior of the calculation caused by resonance excitation. Also presented are 11 measurements from the LLNL EBIT using crystal, grating or the XRS/EBIT microcalorimeter spectrometers, and three measurements from the NIST EBIT using an SAO microcalorimeter. This is a complete version of a figure found in Chen et al. 2006 [80].

Acknowledgements

I would like to acknowledge Peter Beiersdorfer, Klaus Widmann, E. J. Clothiaux, Steve Kahn, Dan Nelson, Ed Magee, Phil D'Antonio, Rich Kelley, F. Scott Porter, Caroline A. Kilbourne, Kevin Boyce, Hui Chen, John Gygax, Duane Liedahl, Ming Feng Gu, Daniel Savin, Daniel Thorn, Mau Chen, Steve Utter, Elmar Träbert, Jeff Van Lue, Ken Visbeck, Kennedy Reed, and Dave Knapp for contributing to this work in a variety of ways. Work by the University of California, LLNL was performed under the auspices of the Department of Energy under contract No. W-7405-Eng-48. Work was also supported by NASA SR & T and APRA grants to LLNL, Columbia University, NASA/Goddard Space Flight Center, and Stanford University.

[1] F. Tyrén. Z. Phys., **111**, 314 (1938).

[2] J. H. Parkinson. Astron. Astrophys., **24**, 215 (1973).

[3] R. L. Blake, T. A. Chubb, H. Friedman, and A. E. Unizicker. Astrophys. J., **142**, 1 (1965).

[4] R. H. Hutcheon, F. P. Pye, and K. D. Evans. Mon. Not. R. astr. Soc., **175**, 489 (1976).

[5] M. Loulergue and H. Nussbaumer. Astron. Astrophys., **24**(1), 209 (1973).

[6] W. M. Neupert, W. Gates, M. Swartz, and R. Young. Astrophys. J. Lett., **149**, L79+ (1967).

[7] G. A. Doschek, J. F. Meekins, and R. D. Cowan. Solar Physics, **29**, 125 (1973).

[8] A. B. C. Walker, Jr., H. R. Rugge, and K. Weiss. Astrophys. J., **192**, 169 (1974).

[9] A. B. C. Walker, Jr., H. R. Rugge, and K. Weiss. Astrophys. J., **194**, 471 (1974).

[10] H. R. Rugge and A. B. C. Walker. Astrophys. J., **219**, 1068 (1978).

[11] H. R. Rugge and D. L. McKenzie. Astrophys. J., **297**, 338 (1985).

[12] K. J. H. Phillips, J. W. Leibacher, C. J. Wolfson, J. H. Parkinson, B. J. Kent, H. E. Mason, L. W. Acton, J. L. Culhane, and A. H. Gabriel. Astrophys. J., **256**, 774 (1982).

[13] K. J. H. Phillips, C. J. Greer, A. K. Bhatia, I. H. Coffey, R. Barnsley, and F. P. Keenan. Astron. Astrophys., **324**, 381 (1997).

[14] K. J. H. Phillips, R. Mewe, L. K. Harra-Murnion, J. S. Kaastra, P. Beiersdorfer, G. V. Brown, and D. A. Liedahl. Astron. Astrophys., **138**(2), 381 (1999).

[15] J. T. Schmelz, J. L. R. Saba, D. Ghosh, and K. T. Strong. Astrophys. J., **473**, 519 (1996).

[16] J. T. Schmelz, J. L. R. Saba, J. C. Chauvin, and K. T. Strong. Astrophys. J., **477**, 509 (1997).

[17] J. L. R. Saba, J. T. Schmelz, A. K. Bhatia, and K. T. Strong. Astrophys. J., **510**, 1064 (1999).

[18] A. K. Bhatia and J. L. R. Saba. Astrophys. J., **563**, 434 (2001).

[19] K. J. H. Phillips, C. J. Greer, A. K. Bhatia, and F. P. Keenan. Astrophys. J. Lett., **469**, L57 (1996).

[20] B. W. Smith, J. C. Raymond, J. B. Mann, and R. D. Cowan. Astrophys. J., **298**, 898 (1985).

[21] J. T. Schmelz, J. L. R. Saba, and K. T. Strong. Astrophys. J. Lett., **398**, L115 (1992).

[22] K. Waljeski, D. Moses, K. Dere, J. L. R. Saba, D. F. Web, and D. M. Zarro. Astrophys. J., **429**, 909 (1994).

[23] A. K. Bhatia and G. A. Doschek. At. Data Nucl. Data Tables, **52**, 1 (1992).

[24] M. Cornille, J. Dubau, P. Faucher, F. Bely-Dubau, and C. Blanchard. Astron. Astrophys.

Supp., **105**, 77 (1994).

[25] P. L. Hagelstein and R. K. Jung. At. Data Nucl. Data Tables, **37**, 121 (1987).

[26] H. L. Zhang, D. H. Sampson, R. E. H. Clark, and J. B. Mann. At. Data Nucl. Data Tables, **37**, 17 (1987).

[27] M. Mohan, R. Sharma, and W. Eissner. Astrophys. J., **108**, 389 (1997).

[28] A. Hibbert, M. L. Dourneuf, and M. Mohan. At. Data Nucl. Data Tables, **53**, 23 (1993).

[29] U. Feldman and L. Cohen. Astrophys. J. Lett., **151**, L55 (1968).

[30] L. R. Cohen and U. Feldman. Astrophys. J. Lett., **160**, L105 (1970).

[31] M. Swartz, S. Kastner, E. Rothe, and W. Neupert. Journal of Physics B Atomic Molecular Physics, **4**, 1747 (1971).

[32] L. F. Chase, W. C. Jordan, J. D. Perez, and R. R. Johnston. pra, **13**, 1497 (1976).

[33] G. E. Bromage, R. D. Cowan, B. C. Fawcett, H. Gordon, M. G. Hobby, N. J. Peacock, and A. Ridgeley. The Laser–produced spectrum of Fe XVII to Fe XXI below 18 Å. Technical Report CLM-R 170, Culham Laboratory, Abingdon, Oxon OX14 3DB (1977).

[34] V. A. Boiko, A. Y. Faenov, and S. A. Pikuz. J. Quant. Spectrosc. Radiat. Transfer, **19**, 11 (1978).

[35] M. J. May, P. Beiersdorfer, J. Dunn, N. Jordan, S. B. Hansen, A. L. Osterheld, A. Y. Faenov, T. A. Pikuz, I. Y. Skobelev, F. Flora, S. Bollanti, P. Di Lazzaro, D. Murra, A. Reale, L. Reale, G. Tomassetti, A. Ritucci, M. Francucci, S. Martellucci, and G. Petrocelli. apjs, **158**, 230 (2005).

[36] P. Beiersdorfer, S. von Goeler, M. Bitter, and D. B. Thorn. Phys. Rev. A, **64**, 032705 (2001).

[37] P. Beiersdorfer, M. Bitter, and S. von Goeler. Astrophys. J., **610**, 616 (2004).

[38] D. W. Savin, P. Beiersdorfer, S. M. Kahn, B. Beck, G. V. Brown, M. F. Gu, D. A. Liedahl, and J. H. Scofield. Rev. Sci. Instrum., **71**(9) (2000).

[39] D. W. Savin, N. R. Badnell, P. Beiersdorfer, B. R. Beck, G. V. Brown, P. Bryans, T. W. Gorczyca, M. F. Gu, S. M. Kahn, J. M. Laming, D. A. Liedahl, W. Mitthumsiri, J. H. Scofield, and K. L. Wong. Can. J. Phys. (2007). These proceedings.

[40] P. Beiersdorfer, L. Schweikhard, J. C. López-Urrutia, and K. Widmann. Rev. Sci. Instrum., **67**(11), 3818 (1996).

[41] L. Schweikhard, P. Beiersdorfer, G. V. Brown, J. R. Crespo López-Urrutia, S. B. Utter, and K. Widmann. Nuclear Instruments and Methods in Physics Research B, **142**, 245 (1998).

[42] G. V. Brown, P. Beiersdorfer, and K. Widmann. Rev. Sci. Instrum., **70**(1), 280 (1999).

[43] P. Beiersdorfer and B. Wargelin. Rev. Sci. Instrum., **65**(1), 13 (1994).

[44] P. Beiersdorfer, R. Marrs, J. Henderson, D. Knapp, M. Levine, D. Platt, M. Schneider, D. Vogel, and K. Wong. Rev. Sci. Instrum., **61**(9), 2338 (1990).

[45] P. Beiersdorfer, E. W. Magee, E. Träbert, H. Chen, K. K. Lepson, M. F. Gu, and M. Schmidt. Rev. Sci. Instrum., **75**(10), 3723 (2004).

[46] F. S. Porter, M. D. Audley, P. Beiersdorfer, K. R. Boyce, R. P. Brekosky, G. V. Brown, K. C. Gendreau, J. Gygax, S. M. Kahn, R. L. Kelley, C. K. Stahle, and A. E. Szymkowiak. In *Proceedings of the 45th annual SPIE meeting on Optical Science and Technology*, page 4140. SPIE Press (2000).

[47] F. S. Porter, P. Beiersdorfer, K. R. Boyce, G. V. Brown, H. Chen, R. L. Kelley, and C. A. Kilbourne. Rev. Sci. Instrum., **75**, 3772 (2004).

[48] F. S. Porter, P. Beiersdorfer, K. R. Boyce, G. V. Brown, H. Chen, J. Gygax, S. M. Kahn, R. L. Kelley, C. A. Kilbourne, E. Magee, and D. B. Thorn. Can. J. Phys. (2007). Submitted.

[49] P. Beiersdorfer. Astron. Astrophys. Review, **41**, 343 (2003).

[50] M. Levine, R. Marrs, D. Knapp, and M. Schneider. Phys. Scr., **T22**, 157 (1988).

[51] R. E. Marrs. *Atomic, Molecular, and Optical Physics: charged particles*, volume 29A of *Experimental Methods in the Physical Sciences*. Academic Press, Inc., San Diego, CA (1995). Chapter 14. Electron Beam Ion Traps.

[52] G. V. Brown, P. Beiersdorfer, S. M. Kahn, D. A. Liedahl, and K. Widmann. Astrophys. J., **502**(2), 1015 (1998).

[53] R. J. Smith, N. S. Brickhouse, D. A. Liedahl, and J. C. Raymond. Astrophys. J. Lett., **556**(2), L91 (2001).

[54] G. V. Brown, P. Beiersdorfer, and K. Widmann. Phys. Rev. A, **63**, 032719 (2001).

[55] H. L. Zhang and D. H. Sampson. At. Data Nucl. Data Tables, **43**, 1 (1989).

[56] G. V. Brown, P. Beiersdorfer, H. Chen, M. H. Chen, and K. J. Reed. Astrophys. J. Lett., **557**, L75 (2001).

[57] M. Laming, I. Kink, E. Takacs, J. V. Porto, J. D. Gillaspy, E. H. Silver, H. W. Schnopper, S. R. Bandler, N. S. Brickhouse, S. S. Murray, M. Barbera, A. k. Bhatia, G. A. Doschek, N. Madden, D. Landis, J. Beeman, and E. E. Haller. Astrophys. J. Lett., **545**(2), L161 (2000).

[58] M. Arnaud and J. Raymond. Astrophys. J., **398**, 394 (1992).

[59] N. S. Brickhouse and J. T. Schmelz. Astrophys. J. Lett., **636**, L53 (2006).

[60] J.-U. Ness, J. H. M. M. Schmitt, M. Audard, M. Güdel, and R. Mewe. Astron. Astrophys., **407**, 347 (2003).

[61] C. R. Canizares, D. P. Huenemoerder, D. S. Davis, K. A. Flanagan, J. Houck, T. H. Markert, H. L. Marshall, M. L. Schattenburg, N. S. Schulz, M. Wise, J. J. Drake, and N. S. Brickhouse. Astrophys. J. Lett., **539**, L41 (2000).

[62] A. C. Brinkman, E. Behar, M. Gudel, A. J. F. den Boggende, G. Braunduardi-Raymont, J. Cottam, C. Erd, J. W. den Herder, F. Jansen, J. S. Kaastra, S. M. Kahn, R. Mewe, F. Paerls, J. R. Peterson, A. P. . Rasmussen, I. Sakelliou, and C. de Vries. Astron. Astrophys., **365**, L324 (2001).

[63] H. Xu, S. M. Kahn, J. R. Peterson, E. Behar, F. B. S. Paerls, R. F. Mushotzky, J. G. Jernigan, and K. Makishima. Astrophys. J., **579**, 600 (2002).

[64] M. Güdel, M. Audard, F. Reale, S. L. Skinner, and J. L. Linsky. Astron. Astrophys., **416**, 713 (2004).

[65] E. Behar, J. Cottam, and S. M. Kahn. Astrophys. J., **548**, 966 (2001).

[66] P. Beiersdorfer, E. Behar, K. R. Boyce, G. V. Brown, H. Chen, K. C. Gendreau, M.-F. Gu, J. Gygax, S. M. Kahn, R. L. Kelley, F. S. Porter, C. K. Stahle, and A. E. Szymkowiak. Astrophys. J. Lett., **576**, L169 (2002).

[67] M. F. Gu. Astrophys. J., **582**, 1241 (2003).

[68] R. Doron and E. Behar. Astrophys. J., **574**, 518 (2002).

[69] G. X. Chen and A. K. Pradhan. Phys. Rev. Lett., **89**(1), 013202 (2002).

[70] G. X. Chen, A. K. Pradhan, and W. Eissner. J. Phys. B, **36**, 453 (2003).

[71] K. B. Fournier and S. B. Hansen. Phys. Rev. A, **71**(1), 012717 (2005).

[72] S. D. Loch, M. S. Pindzola, C. P. Ballance, and D. C. Griffin. Journal of Physics B Atomic Molecular Physics, **39**, 85 (2006).

[73] K. Wong, P. Beiersdorfer, K. Reed, and D. Vogel. Phys. Rev. A, **51**(2), 1214 (1995).

[74] R. Marrs, M. Levine, D. Knapp, and J. Henderson. Phys. Rev. Lett., **60**(17), 1715 (1988).

[75] H. Chen, P. Beiersdorfer, J. H. Scofield, G. V. Brown, K. R. Boyce, R. L. Kelley, C. A. Kilbourne, F. S. Porter, M. F. Gu, and S. M. Kahn. Astrophys. J., **618**, 1086 (2005).

[76] H. Chen, M. F. Gu, P. Beiersdorfer, K. R. Boyce, G. V. Brown, S. M. Kahn, R. L. Kelley, C. A. Kilbourne, F. S. Porter, and J. H. Scofield. Astrophys. J., **646**, 653 (2006).

[77] G. V. Brown, P. Beiersdorfer, K. R. Boyce, H. Chen, R. L. Kelley, C. A. Kilbourne, F. S. Porter, A. E. Szymkowiak, M. F. Gu, and S. M. Kahn. prl, **96**, 253201 (2006).

[78] H. Chen, P. Beiersdorfer, G. V. Brown, K. C. Gendreau, K. R. Boyce, R. L. Kelley, F. S. Porter, C. K. Stahle, A. E. Szymkowiak, S. M. Kahn, and J. Scofield. Astrophys. J. Lett., **567**, L169 (2002).

[79] M. F. Gu, P. Beiersdorfer, G. V. Brown, H. Chen, K. R. Boyce, R. L. Kelley, C. A. Kilbourne, F. S. Porter, and S. M. Kahn. Astrophys. J. Lett., **607**, L143 (2004).

[80] G. X. Chen, K. Kirby, E. Silver, N. S. Brickhouse, J. D. Gillaspy, J. N. Tan, J. M. Pomeroy, and J. M. Lamming. Phys. Rev. Lett., **97**, 143201 (2006).

[81] The OV series satellites were designed to be launch as "piggyback" experiments on Atlas V ICBMs; however, only OVI-1 was actually launched as a "piggyback" experiment. The rest of the OVI satellites were launched on dedicated rockets.

[82] USAF P78-1 was destroyed by the Anti-Satellite (ASAT) weapons program.

[83] *SMM* was repaired in 1984 in flight by the astronauts on board the Challenger Space Shuttle, mission 41-C. Also see http://www.sstd.rl.ac.uk/project/smm/ for more information.